

AUGUST 05 2009

## Robust acoustic particle manipulation: A thin-reflector design for moving particles to a surface

P. Glynne-Jones; R. J. Boltryk; M. Hill; N. R. Harris; P. Baclet



*J. Acoust. Soc. Am.* 126, EL75–EL79 (2009)

<https://doi.org/10.1121/1.3186800>



WE BRING THE NOISE,  
YOU BRING THE PRODUCTS

COMMITTED TO A SMARTER,  
MORE CONNECTED FUTURE

**ETS·LINDGREN**  
An ESCO Technologies Company

# Robust acoustic particle manipulation: A thin-reflector design for moving particles to a surface

**P. Glynn-Jones, R. J. Boltryk, and M. Hill**

*School of Engineering Sciences, University of Southampton, Southampton SO17 1BJ, United Kingdom  
p.glynn-jones@soton.ac.uk; r.j.boltryk@soton.ac.uk; m.hill@soton.ac.uk*

**N. R. Harris**

*Electronics and Computer Science, University of Southampton, Southampton SO17 1BJ, United Kingdom  
nrh@ecs.soton.ac.uk*

**P. Baclet**

*ENSIAME, Université de Valenciennes et du Hainaut Cambrésis, F-59313 Valenciennes, France  
bacletp@orange.fr*

**Abstract:** Existing ultrasonic manipulation devices capable of pushing particles to a surface (“quarter-wave” devices) have significant potential in sensor applications. A configuration for achieving this that uses the first thickness resonance of a layered structure with both a thin reflector layer and thin-fluid layer is described here. Crucially, this mode is efficient with lossy reflector materials such as polymers, produces a more uniform acoustic radiation force at the reflector, and is less sensitive to geometric variations than previously described quarter-wave devices. This design is thus expected to be suitable for mass produced, disposable devices.

© 2009 Acoustical Society of America

**PACS numbers:** 43.25.Qp, 43.20.Ks [AN]

**Date Received:** May 1, 2009     **Date Accepted:** July 1, 2009

## 1. Introduction

Previous literature has described two major classes of planar acoustic particle manipulation devices.

- (a) Those where the dominant resonance is in the fluid layer, leading to agglomeration at one or more pressure nodes within the fluid layer (Hawkes and Coakley, 2001).
- (b) Those where a resonant reflector layer provides a pressure release boundary condition, causing the agglomeration position to occur at a pressure node close to the fluid/reflector interface (Hill, 2003; Hawkes *et al.*, 2004). These devices typically have fluid-layer thickness close to  $\lambda/4$  and reflector thicknesses  $n\lambda/2$ , and are often referred to as “quarter-wave devices.” Quarter-wave devices with no reflector are postulated by Hawkes *et al.* (2002). In their notation, the (non-quarter-wave) device described here is close to “000,” i.e., the carrier, fluid, and reflector layers are all vanishingly thin.

Quarter-wave devices have potential application in sensor technology when combined with surface immunoassays, as the acoustic radiation forces can be used to drive particles of interest, such as bacterial spores (Hawkes *et al.*, 2004; Martin *et al.*, 2005), to an antibody coated sensor surface. Quarter-wave designs have several limitations when used in these applications:

In a conventional design, the radiation force at the fluid/reflector boundary tends to zero. This constraint can be avoided by modifying layer thicknesses (Glynn-Jones *et al.*, 2009); however, it has been observed both in models, and experimentally, that the proximity of the pressure node to the interface can lead to a significantly non-uniform force at the interface. This

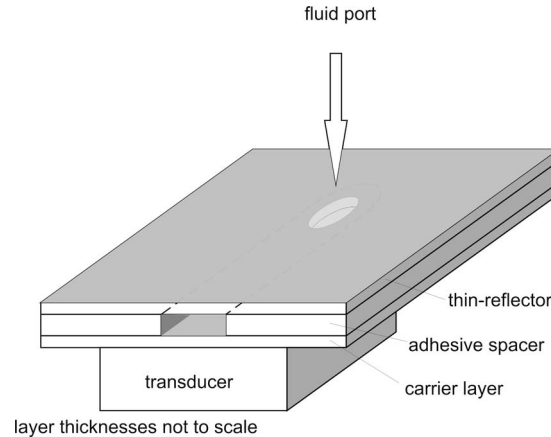


Fig. 1. Thin-reflector device design, showing a cross section across the fluid channel. Particles are driven toward the boundary between the reflector layer and fluid layer.

occurs because lateral variations in the acoustic resonance can distort the expected position of the pressure node sufficiently to cause the node position to be in the reflector in some places and in the fluid in others; thus a particle at the reflector may experience forces either toward or away from the reflector in a single device. Also, this trade-off can cause a pressure anti-node to occur in the channel near the carrier layer, which means that particles near the carrier layer will be driven away from the reflector. In applications where it is required to drive a particle positively onto the reflector surface this limits the effectiveness of such a device.

The resonant nature of the reflector layer in these designs means that a material with a high  $Q$ -factor, such as glass, is usually employed [though designs with polymer layers have been previously reported (Gonzalez *et al.*, 2008)]. In cell-based applications this can lead to significant adhesion if the surface is left untreated. The devices are also sensitive to variations in the layer thicknesses (Townsend *et al.*, 2008).

The authors describe here a new thin-reflector (and thin-fluid) arrangement, shown in Fig. 1, which overcomes the above constraints. It operates at the first thickness resonance of a composite structure consisting of the following layers: transducer (typically lead zirconate titanate, PZT), an optional carrier layer that serves to isolate the transducer from the fluid layer, a fluid layer, and a reflector layer. This leads to pressure nodes at only the air boundaries of the device. By making both the reflector layer and fluid layers much less than a wavelength in thickness, it is found that particles in all parts of the fluid channel are attracted toward the fluid/reflector layer boundary. This configuration has not, to the authors' knowledge, been previously described in a planar manipulation device.

This arrangement also has the advantage that the reflector layer can be thin enough to be compatible with high numerical aperture microscope objectives: important in applications such as bio-sensing and cell handling.

In the modeling below the acoustic radiation force on a particle at points within the fluid is calculated from the following equations derived by Gor'kov (Gor'kov, 1962).

The acoustic radiation force (a time averaged quantity) is given by

$$\langle F(r) \rangle = -\nabla \langle \phi(r) \rangle, \quad (1)$$

where the force potential  $\langle \phi(r) \rangle$  is given by

$$\langle \phi(r) \rangle = -V \left[ \frac{3(\lambda - 1)}{2\lambda + 1} \langle \bar{E}_{\text{kin}}(r) \rangle - \left( 1 - \frac{1}{\sigma^2 \lambda} \right) \langle \bar{E}_{\text{pot}}(r) \rangle \right]. \quad (2)$$

Table 1. Thin-reflector device dimensions and material properties used in finite element modeling.

Layer	Thickness ( $\mu\text{m}$ )	Thickness as a fraction of acoustic wavelength at $f=1.20$ MHz	Material	Model parameters				
				Density ( $\text{kg}/\text{m}^3$ )	Speed of sound ( $\text{m}/\text{s}^2$ )	Young's modulus (GPa)	Poisson's ratio	$Q$ -factor
Transducer	1000	0.27	PZT-26 (Ferropem)	Properties as per manufacturer datasheet				100
Carrier layer	104	0.06	Cellulose acetate	1435	2000	4.38	0.29	30
Fluid	120	0.10	Water	1000	1480	...	...	30
Reflector	104	0.06	Cellulose acetate	As above				

Here  $\lambda$  is the ratio of particle density to fluid density,  $\sigma$  is the ratio of speed of sound in the particle to that in the fluid,  $V$  is the particle volume, and  $\langle \bar{E}_{\text{kin}}(r) \rangle$  and  $\langle \bar{E}_{\text{pot}}(r) \rangle$  are the time averaged kinetic and potential energy densities of the sound wave in the fluid.

## 2. Design, modeling, and results

Whereas the final reflector layer in conventional manipulation devices must have a well controlled thickness to create the necessary boundary conditions for the fluid layer, the final layer in this design can be vanishingly small, and as such the overall acoustic response is not as sensitive to variations in its thickness (a future paper will discuss this in more detail). For clarity, although its function is no longer primarily as a reflector, this layer will continue to be described as “the reflector layer” in this letter.

Table 1 lists the key layer thicknesses, along with the layer thickness as a proportion of the acoustic wavelength in that material at resonance—it is interesting to note how small this proportion is for the fluid and reflector layers. The channel outline was formed by cutting a slot of width 3 mm and length 18 mm into a strip of adhesive transfer tape (3M, 926ATG). This was sandwiched between two squares of cellulose acetate, with fluidic ports at the end of the channel formed by holes in the cellulose acetate. The transducer was a 1 mm thick rectangle ( $8 \times 6 \text{ mm}^2$ ) of PZT26 (Ferropem piezoceramics), and was coupled to the channel with a water soluble ultrasonic coupling gel (Tensive, Parker Laboratories).

The modeled acoustic pressure is distributed across the device as shown in Fig. 2(a). The graph is for an excitation of  $10 \text{ V}_{\text{pp}}$  at the model's resonance frequency of 1.20 MHz. The pressure distribution is calculated using the ANSYS finite element package: The model is essentially one-dimensional, and consists of a strip of elements with boundary conditions to mimic an infinite plain. Table 1 includes the materials data used in the model. Elements capable of modeling both the piezoelectric response to an applied harmonic voltage, and the acoustic/structural interactions are used. The model includes a  $10 \mu\text{m}$  thick gel layer (modeled with the properties of water) between the transducer and carrier layer.

The modeled acoustic radiation force profile on a  $10 \mu\text{m}$  diameter polystyrene bead is shown in Fig. 2(b). It can be seen that at all positions across the channel, there is a force toward the reflector. The magnitude of this force is subject to a large modeling error, as it depends on the damping in the device (results here are for  $Q$ -factors of 100 for the transducer and 30 for subsequent layers), which have been only roughly estimated, and must include corrections to allow for non-parallelisms in the device (Gröschl, 1998).

The electrical input impedance of the assembled device is shown in Fig. 3, where it is compared to the modeled impedance. It can be seen that the actual device exhibits a number of

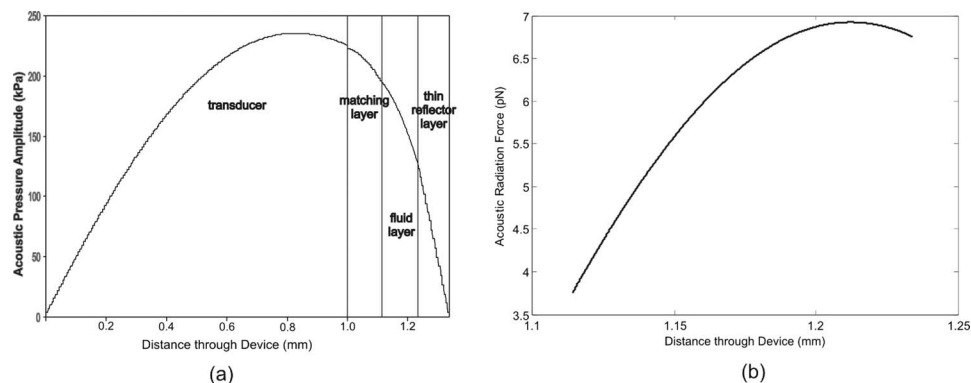


Fig. 2. (a) Acoustic pressure amplitude through the thickness of the device modeled using finite element analysis and (b) acoustic radiation force in the fluid layer on a  $10\ \mu\text{m}$  bead polystyrene bead with a drive voltage of  $10\ \text{V}_{\text{pp}}$ . The positive force indicates a force toward the reflector.

resonances not modeled by the one-dimensional model; it is anticipated that these correspond to lateral acoustic resonances in the transducer. The mode of interest in the device has an impedance minimum at  $1.179\ \text{MHz}$ . Given the estimated nature of the speed of sound in the reflector and carrier layers ( $2000\ \text{m s}^{-1}$ ) and thickness of the gel layer, this is reasonably close to the modeled minimum at  $1.20\ \text{MHz}$ .

To test the device, a dilute solution ( $7.5 \times 10^5$  beads/ml) of polystyrene microspheres of diameter  $10\ \mu\text{m}$  (Polysciences Inc., Fluoresbrite microspheres No. 19096) was flowed through the device driven by a syringe micropump at an average velocity of  $1\ \text{mm s}^{-1}$ . The transducer was driven directly from a signal generator (TTi TG1304) with a sine-wave of frequency  $1.179\ \text{MHz}$  and amplitude  $10\ \text{V}_{\text{pp}}$ . Under these conditions all the beads passing through the device came into contact with the reflector, many of them sticking to it (this was verified visually with a microscope; all free beads could be observed within a single focal plane, and seen moving between and colliding with beads adhered to the reflector surface thus confirming their close proximity to the surface).

To assess the efficiency of the device the acoustic radiation force was balanced against the buoyant weight of the bead (Martin *et al.*, 2005). It was found that the region showing the strongest forces (lateral variations in acoustic force were apparent) would balance a bead at a voltage of  $1.79\ \text{V}$ . Since the force on a bead is proportional to the square of applied voltage, it can be deduced that at  $10\ \text{V}_{\text{pp}}$  drive there is a maximum force of  $8.8\ \text{pN}$  on the bead. This is close to the value predicted by the model [see Fig. 2(b)].

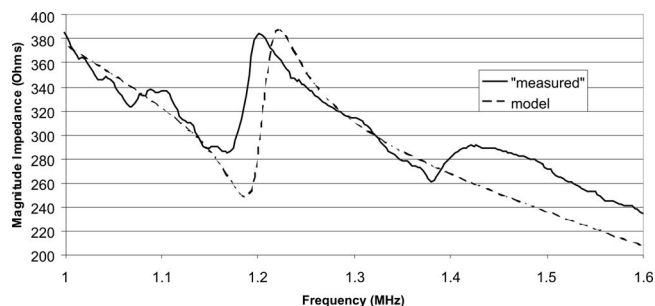


Fig. 3. Device electrical input impedance as measured and modeled. The mode of interest, with a minimum at  $1.179\ \text{MHz}$  in the model, is seen.

### 3. Conclusions

The thin-reflector design successfully manipulates particles into contact with the reflector. In contrast to a quarter-wave design the force at the surface is reliably positive, and less sensitive to small variations in reflector- and fluid-layer thicknesses. The device can be constructed from lossy materials such as plastics, potentially useful for disposable devices, and those where the surface chemistry of glass is unsuitable.

### Acknowledgment

The authors gratefully acknowledge the support of the EPSRC for the project “Ultrasonic manipulation & transport of DNA molecules in evanescent light fields,” Research Grant No. EP/D03454X/1.

### References and links

- Glynn-Jones, P., Boltryk, R. J., Hill, M., Zhang, F., Dong, L. Q., Wilkinson, J. S., Melvin, T., Harris, N. R., and Brown, T. (2009). “Flexible acoustic particle manipulation device with integrated optical waveguide for enhanced microbead assays,” *Anal. Sci.* **25**, 285–291.
- Gonzalez, I., Gomez, T., and Fernandez, L. (2008). “Experimental study of particle motion within a microchannel narrower than half a wavelength,” in *The Sixth USWNet Conference* (ETH, Zurich, Switzerland).
- Gor’kov, L. P. (1962). “On the forces acting on a small particle in an acoustical field in an ideal fluid,” *Sov. Phys. Dokl.* **6**, 773–775.
- Gröschl, M. (1998). “Ultrasonic separation of suspended particles—Part I: Fundamentals,” *Acustica* **84**, 432–447.
- Hawkes, J. J., Gröschl, M., Benes, E., Nowotny, H., and Coakley, W. T. (2002). “Positioning particles within liquids using ultrasound force fields,” *Revista de Acustica* **33**.
- Hawkes, J. J., and Coakley, W. T. (2001). “Force field particle filter, combining ultrasound standing waves and laminar flow,” *Sens. Actuators B* **75**, 213–222.
- Hawkes, J. J., Long, M. J., Coakley, W. T., and McDonnell, M. B. (2004). “Ultrasonic deposition of cells on a surface,” *Biosens. Bioelectron.* **19**, 1021–1028.
- Hill, M. (2003). “The selection of layer thicknesses to control acoustic radiation force profiles in layered resonators,” *J. Acoust. Soc. Am.* **114**, 2654–2661.
- Martin, S. P., Townsend, R. J., Kuznetsova, L. A., Borthwick, K. A. J., Hill, M., McDonnell, M. B., and Coakley, W. T. (2005). “Spore and micro-particle capture on an immunosensor surface in an ultrasound standing wave system,” *Biosens. Bioelectron.* **21**, 758–767.
- Townsend, R. J., Hill, M., Harris, N. R., and McDonnell, M. B. (2008). “Performance of a quarter-wavelength particle concentrator,” *Ultrasonics* **48**, 515–520.